

D42
N79-24043

INVESTIGATION OF ELECTROSTATIC DISCHARGE PHENOMENA ON CONDUCTIVE
AND NON-CONDUCTIVE OPTICAL SOLAR REFLECTORS

S. J. Bosma and C. F. Minier
European Space Research and Technology Centre

and

L. Levy
Département d'Etudes et de Recherches en
Technologie Spatiale

INTRODUCTION

As part of a study of the effects of charge build-up on thermal control coating materials, a sample composed of non-conductive optical solar reflectors (OSR) was irradiated with low energy electrons at the DERTS facility in Toulouse (Ref. 1).

The degradation effects on this panel due to electrostatic discharges justified a follow-up investigation into possible alternatives to limit the amount of damage. This paper evaluates the following systems :

- a) Non-conductive OSR - non-conductive adhesive
- b) Non-conductive OSR - conductive adhesive
- c) Conductive OSR - conductive adhesive (no interconnection of the OSR's)

TEST FACILITY

The tests were performed in an irradiation chamber (Fig. 1) at the DERTS Laboratories in Toulouse. The chamber consists of the following elements :

- A High Tension Feed-Through.

This feed-through is connected to the conductive substrate on which the test sample is glued.

- A Diaphragm

To limit the incident beam on the test sample.

- Three Faraday Cups

To monitor the incident beam during irradiation.

- A Viewing Port

- An Electron Beam Diffusion Window

This window consists of a 2 micron thick aluminium sheet, which permits

the irradiation of large surfaces by diffusion of the initial mono-energetic beam. The obtained flux uniformity over the samples area is $\pm 40\%$.

MEASURED ELECTRICAL PARAMETERS

Leakage Current

The conductive substrate of the test sample is grounded through a series of resistances and a nanoampèremeter (Fig. 2), which measures the leakage current.

Discharge Pulse

An oscilloscope is connected to the resistances in a voltage divider mode (Fig. 2).

A discharge is characterised by comparing the voltage pulses measured over the divider (Figs. 3A and B).

Discharge Current

The substrate of the test sample is directly grounded. The discharge current is measured with a current probe and a fast storage oscilloscope. (Fig. 3C)

Surface Potential

If a test sample is submitted to an electron beam with an energy E_0 and a current I_0 , the actual current I reaching the surface of the test sample will depend on the potential V of this surface.

DERIS have determined the different relations $I(V)$ for various electron beam currents I_0 and energies E_0 .

From these curves the surface potential (V) may be evaluated by measuring the corresponding current (I) at the time of the discharge.

TEST CONDITIONS

A vacuum of better than 10^{-5} torr was maintained during the irradiation.

All samples tested had dimensions of 65 x 65 mm. They were irradiated with electrons of increasing energy, starting from 5 KeV up to 30 KeV with current densities of 0.1 nA/cm^2 to 2 nA/cm^2 until discharges were observed.

When the conditions for electrostatic discharges are obtained, the sample remains irradiated and is allowed to discharge during 6 hours.

GENERAL BEHAVIOUR OF THE IRRADIATED SAMPLE

The impinging electrons on the sample surface cause a charge displacement in the conductive substrate which accounts for the initial high leakage current. This "displacement" current decays with time, because the incident electrons are partially retarded by a potential build-up on the sample surface.

There are two cases to be considered :

case A) (Fig. 4A) The potential build-up is sufficient to decrease the number of incident electrons to a value which can be removed by the leakage paths of the test sample. An equilibrium potential is obtained which is lower than the breakdown voltage of the di-electric.

case B) (Fig. 4B) The charge removal through the leakage paths is at all times smaller than the number of incident electrons. The test sample will charge to the breakdown voltage of the di-electric at which time an abrupt drop in surface potential occurs. It is assumed that this is caused by a discharge of a large surface area. After the discharge the leakage current jumps to a high value and starts to decay until a new discharge takes place.

The discharges described in case B are identified as "large", in contradiction to "small" discharges, which do not considerably modify the surface potential and are assumed to be "point" discharges. This latter type can occur in both cases A and B. These phenomena have been reported by other sources (Refs. 2 and 3).

SYSTEM (a): NON-CONDUCTIVE OSR - NON-CONDUCTIVE ADHESIVE

Test Sample

The sample tested was a panel composed of 9 OSR's manufactured by OCLI, bonded to a rigid plate using RIV 560 (manufacturer : General Electric, USA). This bonding has been done by ERNO, who apply the same procedure to the OTS project. The assembly was mounted onto the test plate at ESTEC, using a conductive adhesive developed by ESTEC which consists of RIV 566 (manufacturer: General Electric, USA) and metal powder 1029B from Chomerics.

Before mounting, the test plate was primed with Dow Corning silicone primer DC 1200. Figure 5 shows the composition of the test panel.

Test Results

A summary of the results obtained from testing the OSR panel is shown by Table I.

Table I

	original	long duration (6 hours)
Irradiation parameter	15 keV, 2 nA	30 keV, 2 nA
Surface potential	4 < U < 9 kV	4 < U < 9 kV
Electrical breakdown	"large and small"	65 large

Investigation of Degradation Effects

This investigation consisted of the following steps :

- 1) photographic examination of 16 pre-determined points (Figure 6); no degradation at first observation
- 2) cleaning with iso propyl alcohol and lens tissues. The sample was examined under grazing incidence. 14 degradation areas were observed with a total area of about 3 mm², i.e. 1.5% of the entire area (Figure 7).

All defects are close to or around defects in the adhesive which were already present before irradiation. It is clear that these points, where RTV is absent or thinner, were weak points because breakdown occurred due to lower insulation resistance.

3) Microscopic investigation.

A Reichert projection microscope was applied working as an interferometer using the Nomarski technique. This technique allows a better visualisation of the defect, but - due to the polarized light - the vertical defects are far more emphasized than the horizontal ones.

At this stage, it was observed that the degradation was a deposit on the surface of the OSR. (Figures 8 and 9)

4) Cleaning with iso propyl alcohol and normal wipe tissues

These tissues which are more abrasive than lens tissues removed the deposit. It should be noticed that the deposit is not soluble in either iso-propyl alcohol or acetone but can be abraded or scratched. An investigation into the bottom layer of the quartz (the silver layer) showed that the silver had not been affected.

5) Reproduction of the defect

A highly powerful electrical breakdown was simulated to recreate the deposit. For this purpose, a "Tesla coil", manufactured by Edwards under the name "H.F. Tester" was used. This instrument supplies a high frequency voltage (0-20 kV) which creates a charge on dielectric material and a discharge through a conductive path mechanism. When such a discharge was applied to the OSR panel, the weak points could easily be seen as a preferred path for discharges.

A first intensive discharge created a deposit comparable to the one obtained in the DERTS test. The silver layer at the bottom was also damaged. (Figure 10)

A similar effect was created when the discharge was initiated in a break line of the OSR itself rather than in the RTV gap. A further analysis of a 15 kV discharge passed through an OSR defect for several seconds revealed a small hole in the top layer together with degradation of the silvered coating in the bottom layer. (Figures 11 and 12)

As only a small deposit on the top layer was observed, it was decided to create a weak discharge with the HF test, but for a longer period of time. A discharge of around 5 kV at a rate of 30 per minute, for 6 hours, was used in the same defect. Little change was observed in the defect in the silver layer, but the deposit on the top layer increased significantly.

6) Interpretation

It is probable that the accumulation of small discharges pyrolyses the silicone adhesive (RTV 560) and gives rise to a projection of silica particles which deposit on the top layer..

Summary

- 1) After irradiation at DERTS, no degradation of the silver layer had occurred;
- 2) At the weak points, with respect to breakdown resistance, a deposit is formed which is probably silica;
- 3) The changes in thermo-optical properties due to these deposits should be rather low (a few percent increase in α , but perhaps also in ϵ);
- 4) The amount of these deposits should increase with an increasing number of discharges;
- 5) If a large breakdown occurs, it will affect the bottom layer of silver, but the size of the defect will probably not increase with the number of discharges. Microscopic investigations show, however, that the aluminium layer of the substrate is more severely attacked;
- 6) It seems that any failure in the OSR is a privileged area as regards the likely occurrence of a discharge;
- 7) It seems reasonable to suppose that, with a conductive binder, this sort of defect will not appear.

SYSTEM (b): NON-CONDUCTIVE OSR - CONDUCTIVE ADHESIVE

Test Sample

In accordance with Point 7 of the summary of the previous test, DERTS have performed a second test on 9 OCLI OSR's bonded directly onto a test plate with a conductive adhesive developed by ESTEK Materials Section and consisting of RTV 566 with metal powder 1029B from Chemerics. (Ref. 4) Before mounting, the test plate was primed with Dow Corning silicone primer DC 1200.

Test Conditions

The test conditions were similar to those applied to the previous test. The sample was irradiated with electrons of increasing energy, starting from 15 KeV up to 30 KeV with current densities of 1 nA/cm² to 2 nA/cm².

Test Results

A summary of the results from testing the OSR panel is shown in Table II. The first discharges started at 20 KeV and 1 nA/cm², whereas in the previous test, the discharges commenced at 25KeV and 2nA/cm². This could be due to the fact that one of the OSR's was broken. A photographic investigation during the test showed that the crack was a preferential path, but not the only one. (Figure 13).

Furthermore the breakdown limit of the sample appeared to decrease after longer irradiation periods. At the beginning of the test, there were no discharges at 15 KeV electron irradiation, but at the end of the test sequence, there were 2 "large" discharges at this level. If the irradiation time had been extended, more discharges would have occurred. The sample was however constrained to the same irradiation time as the previous sample for comparison.

Investigation of Degradation Effects

Prior to cleaning the panel the surfaces of the OSR have been examined, using the same technique with the Reichert microscope.

- The observation shows that, on the front layer, there is a faint deposit of microscopic particles; again projection of silica, but a smaller amount than previously observed.

- The bottom layer of the OSR (the silver layer) is more severely damaged along the border line. Cracks in the silver layer appear which are in the order of 0.2 mm diameter. (Figure 14).

- In addition, a lot of micro spots (0.02 mm in diameter) of burnt silver in the middle of the OSR itself were visible.

- In another place, these micro spots have generated a blistering effect on the silver layer in a larger area (0.1 mm diameter). In this case, the front layer shows no defect at all.

On the previously cracked OSR, holes have been created between the front layer and the bottom layer, with demetallisation. This phenomenon had been predicted and analysed in the previous test. (Figure 15)

Interpretation

It was difficult to find a plausible explanation for the unexpected behaviour of the non-conductive OSR with conductive adhesive. Instead of diminishing the degradation effects of the OSR, increased damage in the silver layer was introduced. The missing link was found when information was received that the OLI OSR's have a non-conductive layer (silicium-oxide and an organic finish) on the backside. A electrical resistance check with an Ohm-meter showed that the backside was indeed non-conductive.

The following discharge mechanisms could be adapted after this new development was introduced. (Figure 16).

In the case of a conductive adhesive a leakage current will flow from the front face to the metal layer on the back of the OSR due to the conductivity of the adhesive. A differential voltage will appear between the silver layer and the non-conductive silicon-oxide layer. A discharge from the silver layer will occur when the breakdown voltage of the silicon-oxide layer is exceeded. This will cause fusing and vapourisation of micro spots of silver.

The question arises : "Why this phenomenon does not appear when the non-conductive adhesive is used?" A possible answer is that, as shown in the previous test, a breakdown was created preferably at a defect in the adhesive layer. In this case, the silver is not a preferential path because it is completely insulated by a non-conductive layer on either side.

Summary

- After irradiation at DERTS, the silver layer was seen to be damaged (edges and micro spots).
- There was little or no deposit of silica on the front layer.
- The degradations of the silvered layer are small in area and at this point cannot change significantly the thermo-optical properties of the OSR, but they would be cumulative during life.
- As previously observed, cracks in the OSR are preferential areas of degradation and shall not be tolerated in spacecraft design.

INTERMEDIATE REVIEW

With the introduction of a new dimension due to the non-conductive backlayer of the OCL1 OSR's, the range of three types of systems has been extended to four types (see Figure 17).

- | | | | |
|----|-----|---|---------------------------|
| a) | OSR | non-conductive front layer
non-conductive back layer | - non conductive adhesive |
| b) | OSR | non-conductive front layer
non-conductive back layer | - conductive adhesive |
| c) | OSR | conductive front layer
conductive back layer | - conductive adhesive |
| d) | OSR | non-conductive front layer
conductive back layer | - conductive adhesive |

SYSTEM (c) : - BOTH SIDES CONDUCTIVE OSR - CONDUCTIVE ADHESIVE
(no interconnection on the front face)

Test Sample

A third test was performed on 4 PPE OSR's with the conductive adhesive described in the previous test. The top surface of the OSR is coated with indium-oxide which is a conductive medium. Moreover, the rear side of the

PPE OSR is not coated with a non-conductive layer.

The sample was composed of three mirrors of 40 x 20 mm and one mirror of 40 x 15, which was intentionally broken. (Figure 18) The dimensions of the substrate were again 65 x 65 mm.

Test Conditions

The test conditions were similar to those used for the two previous tests. The sample was irradiated with electrons of increasing energy, starting from 20 KeV up to 30 KeV with current densities of 1 nA/cm² to 10 nA/cm².

Test Results

A summary of the results of the test on the OSR panel is given in Table III.

The surface potential of the sample was low, which indicates a high leakage current. No discharges were noticed below incident electrons of 30 KeV energy.

When the flux was increased to 2 nA/cm², very small discharges appeared at the beginning of the irradiation, but their number decreased during irradiation.

At a flux of 4 nA/cm², the same phenomenon was noticed, but the number of discharges did not decrease as rapidly as at the 2 nA/cm² flux level.

At a flux level of 10 nA/cm², there were a number of small discharges at the start of irradiation, but after 24 hours they had disappeared. A fluorescence effect was observed on the OSR during electron impact, however, this effect disappeared as soon as the electron beam was interrupted.

Investigation into Degradation Effects

Prior to cleaning the panel, we have examined the surfaces of the OSR, using the same technique as before with the Reichert microscope. No degradation was observed either as projection of silica or damage in the silver layer. The cracks which had been caused before the irradiation test showed no degradation effects.

The conductive backside of the PPE OSR brings about that the silver layer does not not accumulate charge while the indium-oxide achieves the same effect for the top layer.

In how far the indium-oxide layer is necessary will be investigated in a fourth test planned in the future on the system :

OSR	non-conductive front layer	-	conductive adhesive
	conductive back layer		

The effects may be less serious than expected. As was indicated by the second test with the OCLI OSR and conductive adhesive, the most severe degradation occurred in the silver layer which was caused by the non-conductive layer on the backside of the OSR. This would not be the case with PPE OSR's which have a conductive backside.

CONCLUSION

The implications of this paper are very important. It has been proven that a combination of a both sides conductive OSR with a conductive adhesive shows no visible degradation during the irradiation tests performed.

In contradiction, a non-conductive OSR with a conductive or non-conductive adhesive shows degradation effects which could accumulate to hazardous proportions during life.

In particular, the non-conductive backside of the OCLI OSR causes defects in the intermediate silver layer in combination with a conductive adhesive.

Apart from the electrostatic charging advantages of the conductive OSR with conductive adhesive, the application and financial aspects should not be underestimated. In combination with a conductive adhesive, interconnecting pads between the conductive OSR's individually and to ground would not be necessary. These pads are very fragile and tend to break easily. In the past, they have given rise to many problems. OSR's with conductive pads are considerably more expensive than standard types.

Additionally, a great many man-hours, now required for very delicate interconnection work, may be saved.

REFERENCES

1. Irradiation par Electrons de Revêtement de Contrôle Technique.
Report on work performed by DERTS under ESA contract No. 2638/76.
2. Stevens, N.J., Lovell, R.R. and Gore, V : Spacecraft Charging
Investigation for the CTS Project. NASA TMX-71795, June 1975.
3. Pike, L.P. and Lovell, R.R. : Proceedings of the Spacecraft Charging
Technology Conference. NASA TMX-73577, February 1977.
4. Froggatt, M. and Gourmelon, G. : Evaluation of Three Conductive Adhesives
for Use on ECS. ESA E.W.P. 1010, May 1976.

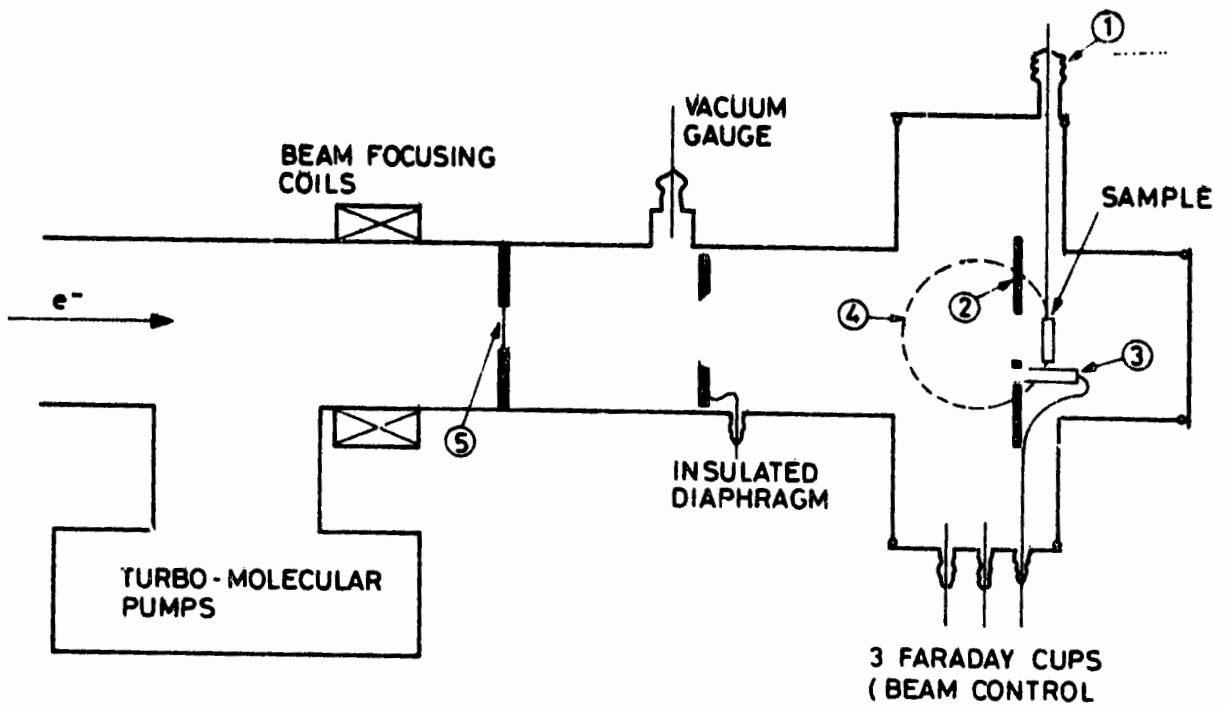
TABLE II

Electron Energy	Electron Flux	Irradiation time	Discharge		Discharge Rate	Surface Potential at Time of Discharge	Number of Discharges over 6 hours	Remarks
			Small	Large				
15 keV	1 nA/cm ²	30 min						No discharging
20 keV	1 nA/cm ²	80 min	Yes	Yes	5min to 7min	6 kV*	60	surface potential 5.5 kV
25 keV	1 nA/cm ²	36 min	Yes	Yes	4min	5.4 kV*	90	
20 keV	1 nA/cm ²	86 min	Yes	Yes	3½ min to 4½ min	4.5 kV*	90	Irradiation stopped after ½ hr. due to instability. Irradiation continued with lower energies
25 keV	1 nA/cm ²	25 min	Yes	Yes	3½ min	4.4 kV*	100	
25 keV	2 nA/cm ²	21 min	Yes	Yes	1½ min	4 kV*	240	
30 keV	1 nA/cm ²	44 min	Yes	Yes	3min	4.7 kV*	120	Time between two irradiations: 15hrs.
30 keV	2 nA/cm ²	40 H	Yes	Yes	1½ min to 2 min	4.6 kV*	200	
15 keV	1 nA/cm ²	45 min	Yes	Yes	15 to 20min	7.5 kV	20	Measurements are based on two discharges

* Values are based on a large number of discharges.

TABLE III

Electron Energy	Electron Flux	Irradiation Time	Observations
20 keV	1 nA/cm ²	20 min	None
30 keV	1 nA/cm ²	20 min	None
30 keV	2 nA/cm ²	25 min	Numerous small discharges during the first 5 minutes
30 keV	4 nA/cm ²	8 hours	Numerous small discharges during the first hours (several discharges per minute). Still some discharging at the end of the irradiation
30 keV	10 nA/cm ²	24 hours	Very small discharges at the start of the irradiation - no discharging at the end.



- ① HIGH TENSION FEED-THROUGH
- ② DIAPHRAGM
- ③ FARADAY CUP
- ④ VIEWING PORT
- ⑤ ELECTRON-BEAM DIFFUSION WINDOW

FIG.1 EXPERIMENTAL SET-UP

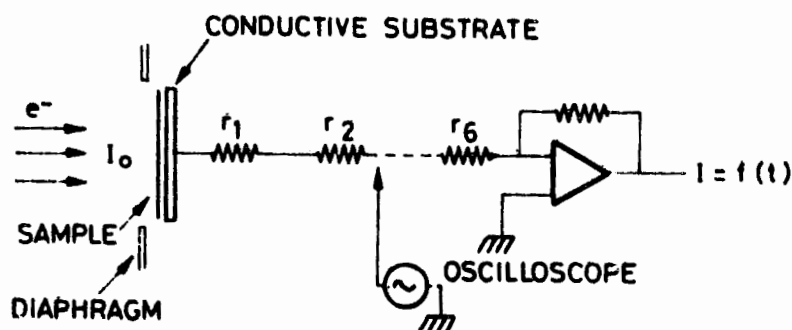
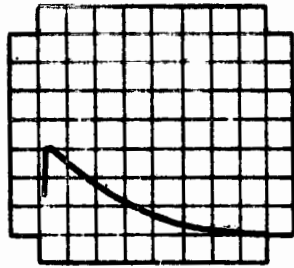
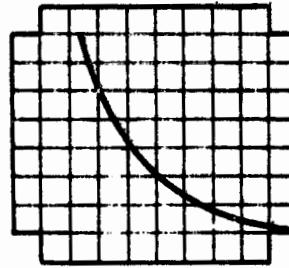


FIG.2 MEASUREMENT SYSTEM



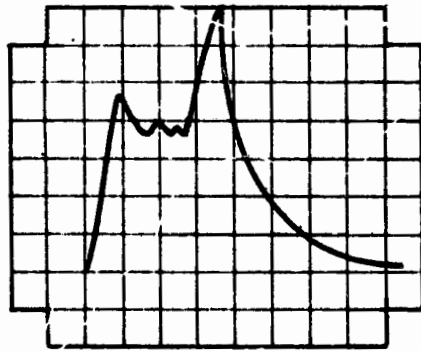
AFTER 21H
IRRADIATION



AFTER 26H
IRRADIATION

OSR
MIRRORS 20 x 20 (9)
30 keV - 2 nA/cm² $R = \frac{110}{11000}$
50V/cm, 100 μs/cm

FIG.3 A AND B TYPICAL VOLTAGE PULSES



OSR
MIRRORS 20x20 (9)
30 keV - 2 nA/cm²
5 A / DIV.
50ns / DIV.

FIG.3 C A TYPICAL DISCHARGE CURRENT PULSE

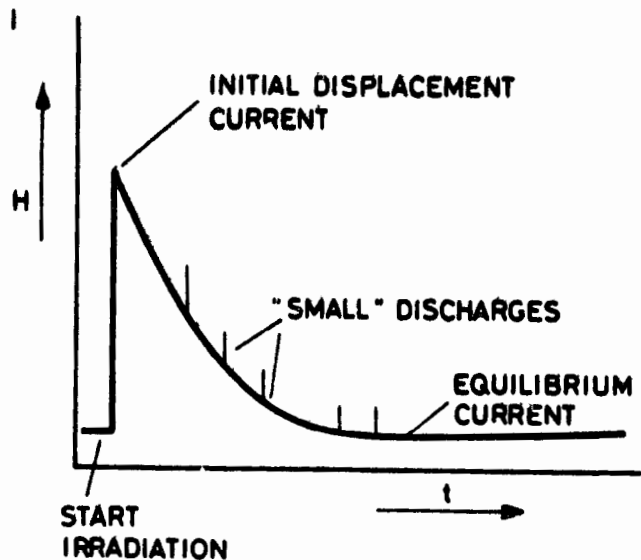


FIG. 4A CASE A

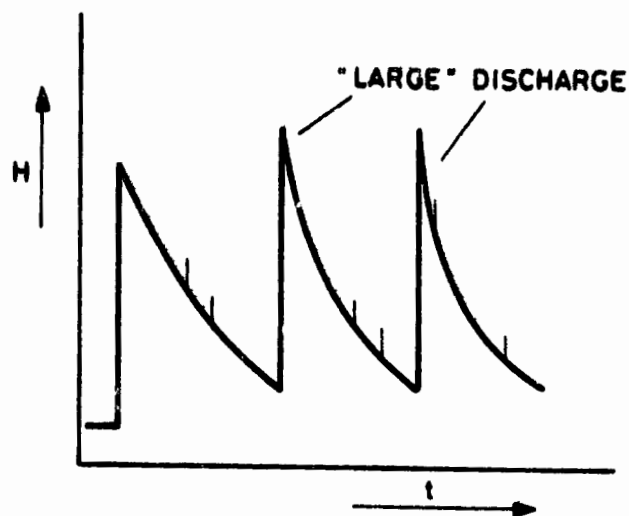
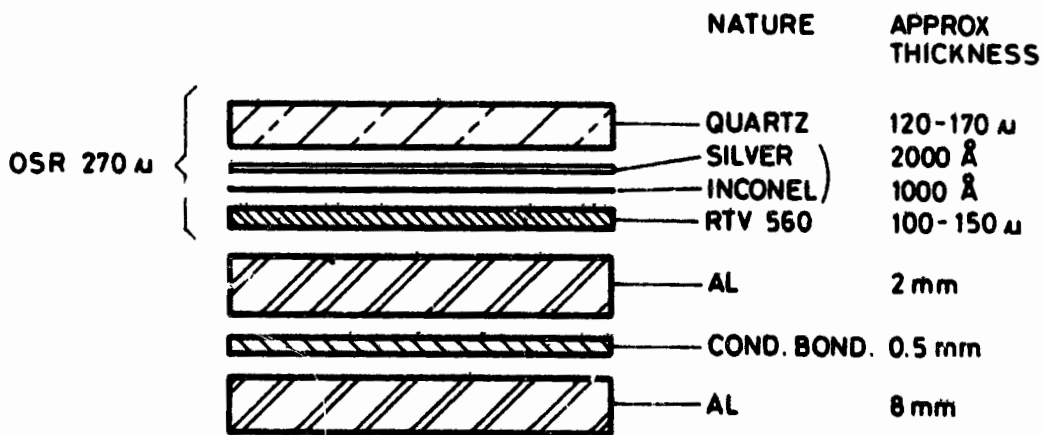


FIG. 4B CASE B



* ASSUMED

FIG. 5 NON-CONDUCTIVE OSR -
NON-CONDUCTIVE ADHESIVE

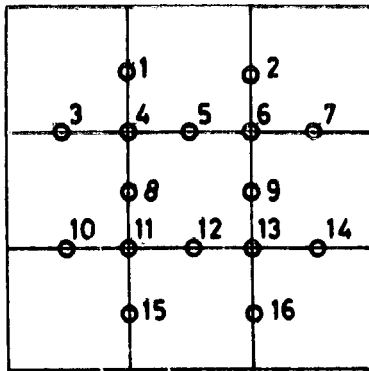


FIG.6 PRE- DETERMINED EXAMINATION POINTS

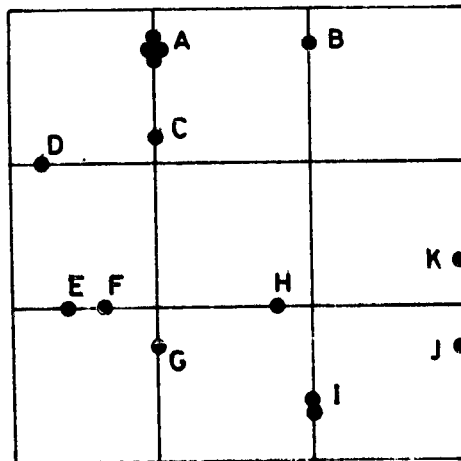


FIG.7 DEGRADED AREAS

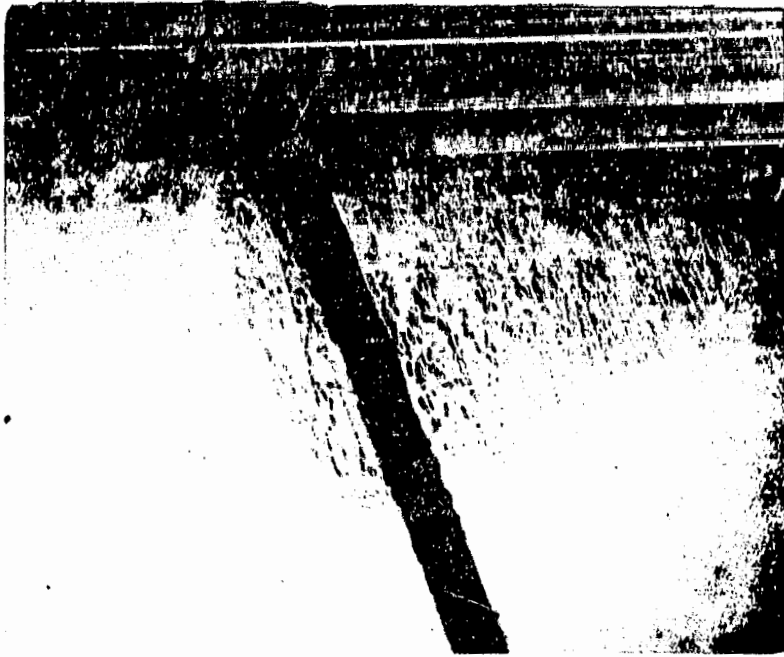


FIG.8 DEFECT AT POINT H (x30)



FIG.9 SAME DEFECT AS IN FIG.8 BUT AT HIGHER
MAGNIFICATION (x 300)

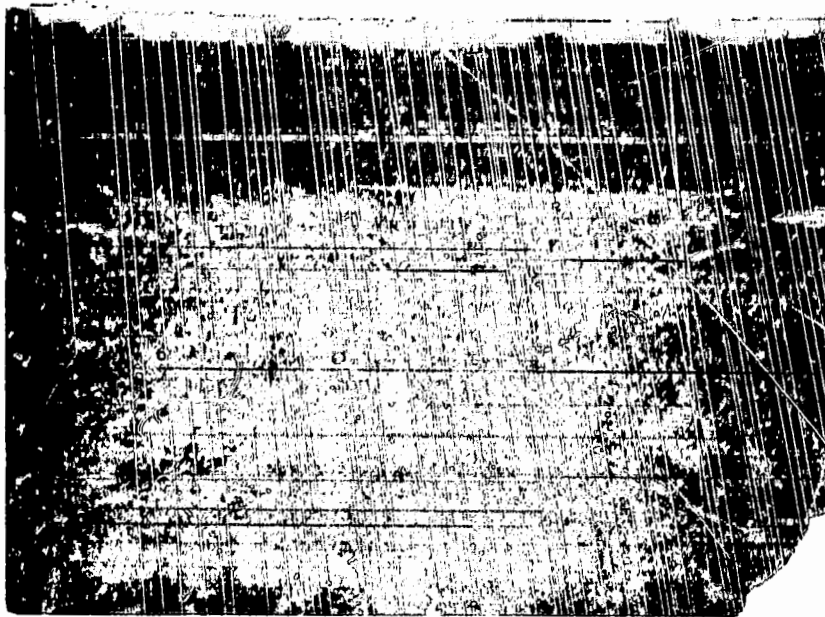
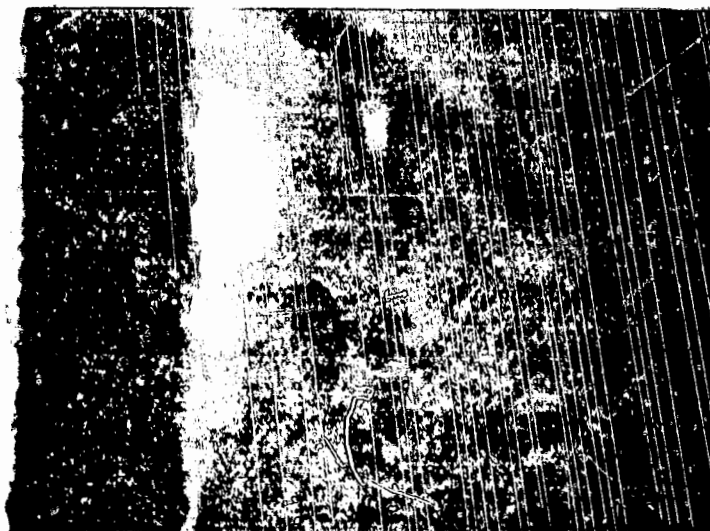


FIG.10 BREAKDOWN CREATED BY HF CHANGE IN SILVER LAYER



ORIGINAL PAGE IS
OF POOR QUALITY

FIG.11 BREAKDOWN IN THE QUARTZ ITSELF TOP LAYER

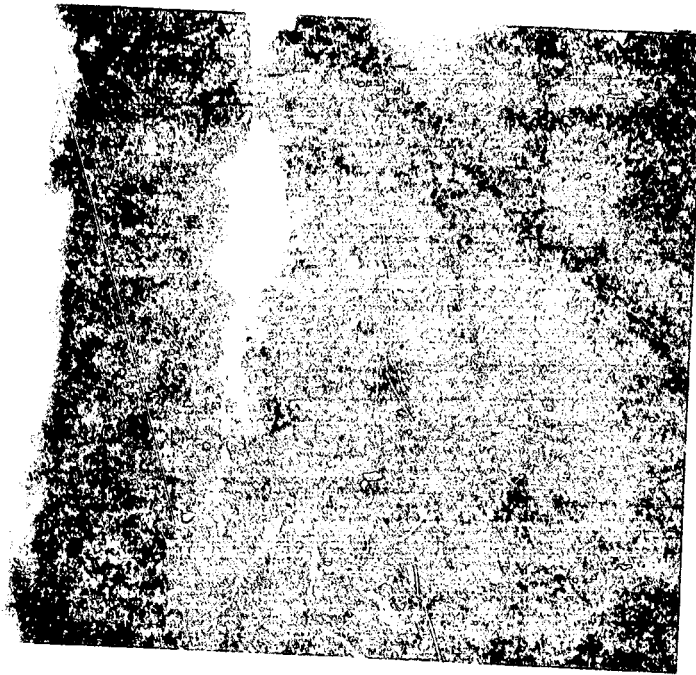


FIG.12 AS FIG.11 BUT SHOWING BOTTOM LAYER

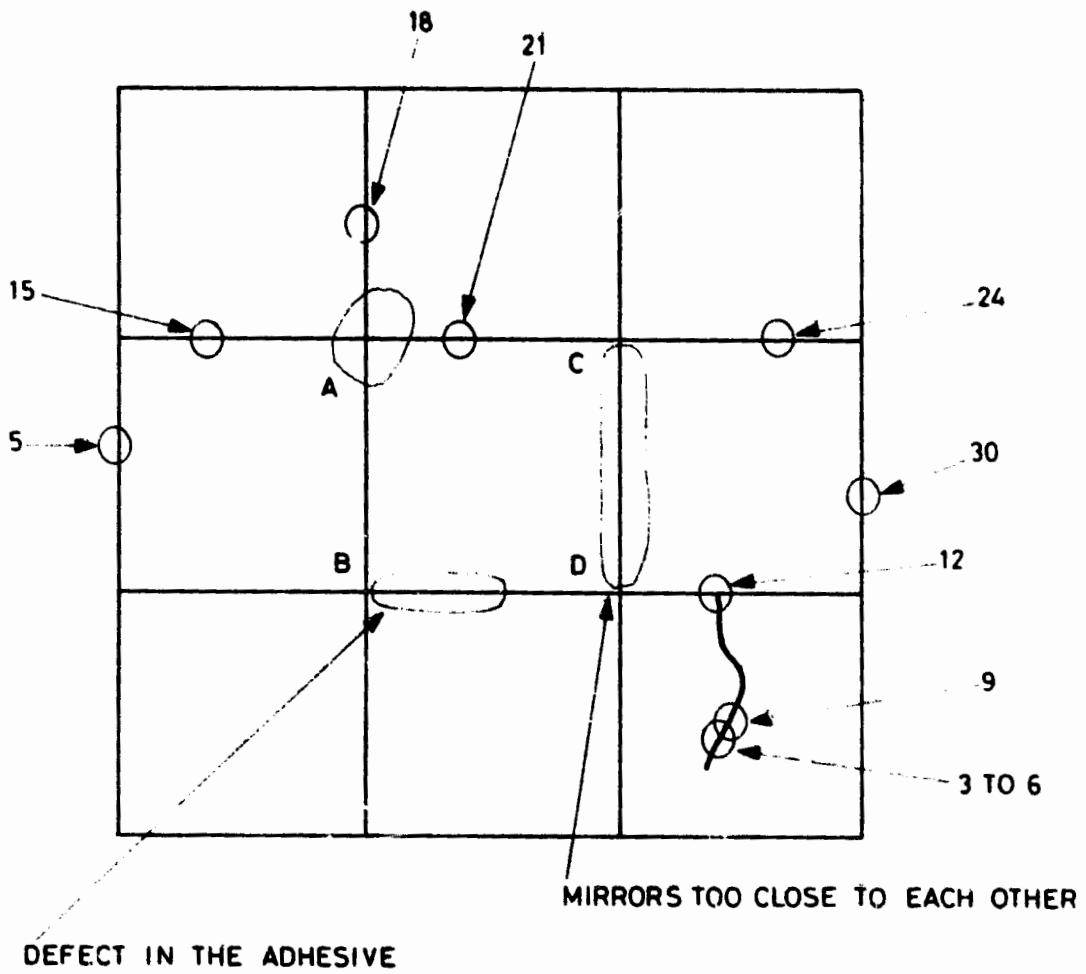


FIG. 13 DEGRADED AREAS ON OCLI OSR'S
WITH CONDUCTIVE ADHESIVE



FIG.14 DEFECT IN THE SILVER LAYER (x125)



FIG.15 DEFECT IN PREVIOUSLY CRACKED OSR

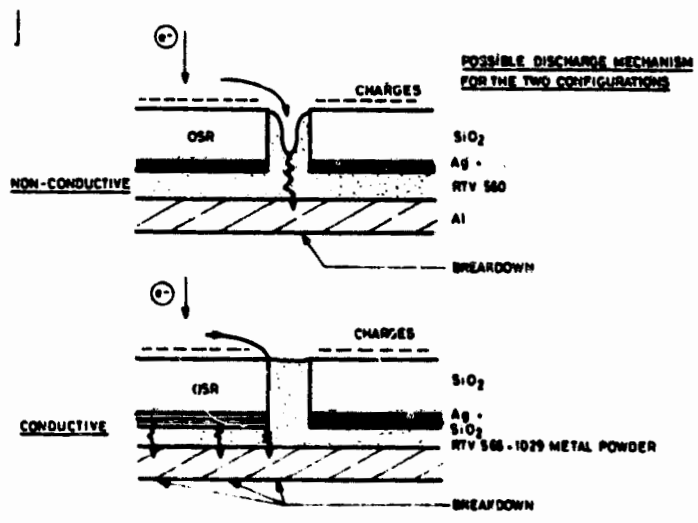


FIG.16 POSSIBLE DISCHARGE MECHANISMS IN OSR'S

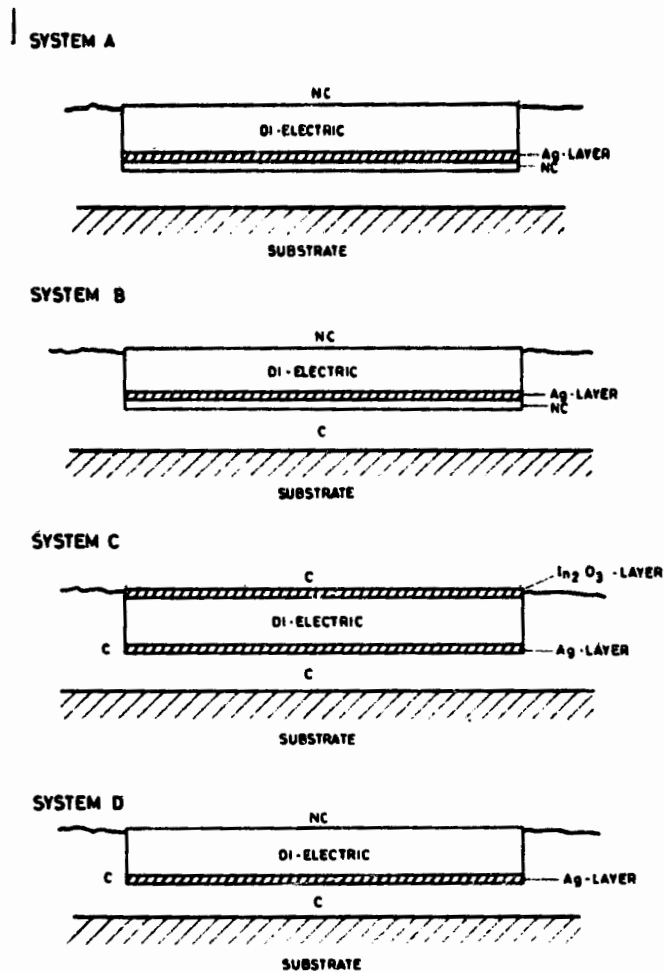


FIG.17 TESTED SYSTEMS

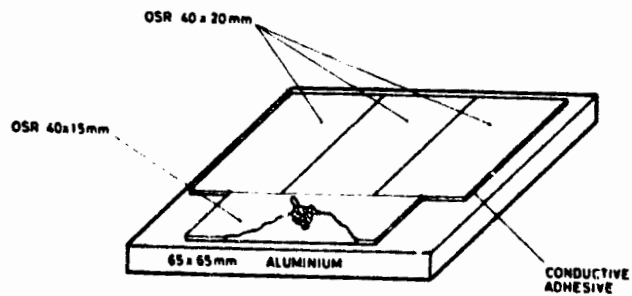


FIG.18 CONDUCTIVE PPE OSR WITH CONDUCTIVE ADHESIVE